Available online at www.sciencedirect.com
ScienceDirect
Journal of Hazardous Materials 154 (2008) 1183–1191
Journal of Hazardous Materials
www.elsevier.com/locate/jhazmat

Adsorption characteristics of acetone, chloroform and acetonitrile on sludge-derived adsorbent, commercial granular activated carbon and activated carbon fibers

Tsai Jiun-Horng [a], Chiang Hsiu-Mei [b], Huang Guan-Yinag [c], Chiang Hung-Lung [d,*]

[a] *Department of Environmental Engineering, Sustainable Environment Research Center, National Cheng-Kung University, Tainan, Taiwan*
[b] *Department of Cosmeceutics, China Medical University, Taichung, Taiwan*
[c] *Department of Environmental Engineering, Fooyin University, Kaohsiung, Taiwan*
[d] *Department of Health Risk Management, China Medical University, Taichung 40402, Taiwan*

Received 22 August 2007; received in revised form 9 November 2007; accepted 9 November 2007
Available online 23 November 2007

Abstract

The adsorption characteristics of chloroform, acetone, and acetonitrile on commercial activated carbon (C1), two types of activated carbon fibers (F1 and F2), and sludge adsorbent (S1) was investigated. The chloroform influent concentration ranged from 90 to 7800 ppm and the acetone concentration from 80 to 6900 ppm; the sequence of the adsorption capacity of chloroform and acetone on adsorbents was F2 > F1 ∼ C1 ∼ S1. The adsorption capacity of acetonitrile ranged from 4 to 100 mg/g, corresponding to the influent range from 43 to 2700 ppm for C1, S1, and F1. The acetonitrile adsorption capacity of F2 was ∼20% higher than that of the other adsorbents at temperatures <30 °C. The Freundlich equation fit the data better than the Langmuir and Dubinin–Radushkevich (D–R) equations. The adsorption rate of carbon fibers is higher than that of the other adsorbents due to their smaller fiber diameter and higher surface area. The micropore diffusion coefficient of VOC on activated carbon and sludge adsorbent was $\sim 10^{-4}$ cm^2 s^{-1}. The diffusion coefficient of VOC on carbon fibers ranged from 10^{-8} to 10^{-7} cm^2 s^{-1}. The small carbon fiber pore size corresponds to a smaller diffusion coefficient.

Keywords: Activated carbon; Sludge adsorbent; Chloroform; Acetonitrile; Acetone

1. Introduction

Many VOCs are hazardous to human health and the environment. Adsorption is one of the most practical methods for separating and recovering VOCs from industrial flue gas streams. Many adsorbents have been developed in recent years to improve adsorption performance. Activated carbon fiber and granular activated carbon are popular adsorbents used to remove VOCs from the gas stream. Recently, VOCs have also become an important issue for indoor air quality, which is a public concern, and adsorption is one of the selected control technologies. Chloroform and acetonitrile are produced and used in industry and the laboratory, posing a threat to those working in the VOC-contaminated atmosphere. Therefore, VOC exhaust control is important to indoor air quality.

Chloroform can be adsorbed by activated carbon [1], silicate, and dealuminated zeolite Y [2]. In addition, acetonitrile can be removed by activated carbon [3]. But little research has focused on the adsorption of chloroform and acetonitrile using activated carbon fiber (ACF).

Some biomass materials can be used as raw materials of activated carbon, e.g., evergreen oak, bamboo, coconut shell, and Japanese cedar. These adsorbents have been used to remove chloroform and other organic matter from drinking water [4]. In addition, after proper treatment, sludge can be used to produce an adsorbent for VOC and H_2S control [5–7]. Biomass reuse should be considered for the sustainable preservation and protection of the environment.

Some advantages of ACF are the smaller fiber diameter, more concentrated pore size distribution, and excellent adsorp-

* Corresponding author. Tel.: +886 4 22079685; fax: +886 4 22079687.
E-mail address: hlchiang@mail.cmu.edu.tw (H.-L. Chiang).

0304-3894/$ – see front matter © 2007 Elsevier B.V. All rights reserved.
doi:10.1016/j.jhazmat.2007.11.065

tion capacity at low adsorbate concentrations compared with traditionally activated carbons [8,9]. Generally, ACF is a kind of micropore carbonaceous adsorbent associated with slit-shaped pores [9,10]. The adsorption rate could be increased substantially by using narrow-diameter activated carbons such as ACF, which exhibits rapid intraparticle adsorption kinetics in gas and liquid-phase adsorption because of its thin fibrous shape [11]. Furthermore, ACF activated by normal steam or CO_2 is hydrophobic and does not show ideal adsorption capacity for polar or polarizable molecules. Hashiho et al. [12] successfully used activated carbon fiber cloth to capture VOCs and HAPs from the air stream; the cloth could be regenerated using a microwave-swing system. ACF is an important material used in high-efficiency filtration systems for indoor air quality control.

In this study, sludge-derived adsorbent (S1), commercial activated carbon (C1), and two types of activated carbon fibers (F1 and F2) were used to investigate the adsorption characteristics of acetone, chloroform, and acetonitrile. The physical characteristics, surface oxygen functional groups, pH, and ash content of various adsorbents were analyzed in this study. In addition, the adsorption capacity and diffusion coefficient of adsorbate that adsorbed on different adsorbents were surveyed. Therefore, this study could provide detailed and comprehensive data for use in adsorption process design.

2. Experimental

2.1. Adsorbents

Four kinds of adsorbents – commercial activated carbon (C1), activated carbon fibers (F1 and F2), and sludge adsorbent (S1) – were selected for adsorption of chloroform, acetonitrile and acetone. Steam activation of select grades of coal was used to produce C1 (Norit GAC 830, Netherlands). S1 was made of biosludge obtained from the wastewater treatment plant of a petrochemical industry in Kaohsiung, Taiwan, activated by 1.0 M $ZnCl_2$, and pyrolyzed at 500 °C for 30 min [13]. The particle size of the granular adsorbent ranged from 1.68 to 2.0 mm (mesh 10–12). F1 was polyacrylonitrile (PAN), AT0902, made by KoTHmex, Taiwan Carbon Technology Co. Ltd. F2 (CARBOFLEX, Anshan East Asia Carbon Fibers Co. Ltd.) was generated from pitch. F1 and F2 were 7 and 18.8 μm in diameter (the microscopy was used for the measurement of diameter), respectively.

2.2. SEM photograph

To better understand the surface structure, photomicrographs of the surface of these adsorbents were obtained by scanning electron microscope (SEM, XL-40FEG, Philip).

2.3. Surface area, pore volume distribution

The physical characteristics of the adsorbents, including the specific surface area, pore volume distribution, and pore diameter, were measured via N_2(g) adsorption in an ASAP 2010 micropore analyzer at 77 K in liquid N_2. The surface area was calculated by the Brunauer–Emmett–Teller (BET) method [14]. Total pore volume and micropore volume were measured by the Barrett–Joyner–Halenda (BJH) method and the *t*-plot and Harkins-Jura methods, respectively [15–17]. Silica–alumina (surface area: 215 ± 6 m^2/g, total pore volume: 0.61 ± 0.08 cm^3/g, average pore diameter: 114 ± 15 Å), alumina (multipoint specific surface area: 0.51 ± 0.03 m^2/g), and molecular sieve (median pore diameter: 8.3 ± 0.2 Å) were obtained from Micromeritics and used for quality assurance and quality control. Five samples were taken for each adsorbent, and analysis of each sample was duplicated.

2.4. Ash content

Ash content in the adsorbent was analyzed according to ASTM D2866-94. The crucible was preheated in a furnace at 650 ± 25 °C for 1 h and then cooled down to room temperature and weighed (W_0). Next, the adsorbent was added into the crucible, and its weight was calculated (W_1). Then the crucible was placed in the oven, with the temperature maintained at 105 °C for 30 min and then raised to 650 ± 25 °C and maintained for 16 h. Finally, the crucible was placed in a desiccator for conditioning, and its weight was determined (W_2).

$$\text{Ash}\,(\%) = \frac{W_2 - W_0}{W_1 - W_0} \times 100 \quad (1)$$

2.5. pH of adsorbent

ASTM D3838-80 was used as a reference to determine the pH of adsorbents. The adsorbent was placed into the cuvette, and 20 ml of boiling water was added. Then, the boiling condition was maintained for 15 min, after which the water was cooled down to measure the pH.

2.6. Boehm titration

Procedures for the analysis of oxygen functional groups followed the method established by Boehm [18]. The activated carbon samples were first dried in a vacuum oven (10^{-2} to 10^{-3} mmHg, 105 °C) for 24 h. Twenty-five millilitres of an alkali solution (0.1 N $NaHCO_3$, Na_2CO_3, and NaOH) was added to test tubes containing a given amount of the activated carbon sample (1–5 g). The samples were constantly mixed over a vibrator (100 rpm) at 25 °C for 24 h. A given amount of the supernatant (5 mL) was drawn from the test tubes and back titrated with HCl (0.1 N) solution. The concentrations of various functional groups were determined by the residual bases after back titration as described by Boehm [18–20].

2.7. Adsorption kinetic

Procedures for kinetic adsorption experiments and related adsorption conditions were as follows. A given amount (50–100 mg) of adsorbent was placed in an electrical balance that was connected to a data-acquisition system. The influent concentration of chloroform was set at a range from 90 to

7800 ppm, acetone from 80 to 6900 ppm, and acetonitrile from 43 to 2700 ppm. The inflow rate of chloroform and acetonitrile vapor was set at 1.0 L/min, the adsorption temperature ranged from 10 to 80 °C, and the temperature variation was less than 0.1 °C. The kinetic adsorption runs were repeated five times for all experimental concentrations.

2.8. Diffusion coefficient of chloroform and acetonitrile

The micropore diffusion was derived as follows [21]:

$$\frac{\partial q}{\partial t} = \left(\frac{1}{r^2}\right) \frac{\partial(r^2 D_c(\partial q/\partial r))}{\partial r} \tag{2}$$

Assuming D_c is constant, Eq. (2) can be derived as Eq. (3):

$$\frac{\partial q}{\partial t} = D_c \left(\frac{\partial^2 q}{\partial r^2} + \left(\frac{2}{r}\right)\frac{\partial q}{\partial r}\right) \tag{3}$$

where r is the distance normal to the external surface, D_c is the intracrystalline diffusivity, and $q(r, t)$ is the amount adsorbed at time = t. The initial and boundary condition are as follows:

$$q(r,\ 0) = q_0, \qquad q(r_c, t) = q_t, \qquad \left(\frac{\partial q}{\partial r}\right)_{r=0} = 0$$

then

$$\frac{(\bar{q} - q_0)}{(q_t - q_0)} = \frac{M_t}{M_\infty} = 1 - \left(\frac{6}{\pi^2}\right) \sum_{n=1}^{\infty} \frac{1}{n^2} \exp\left(\frac{-n^2\pi^2 D_c t}{r_c^2}\right) \tag{4}$$

where $\bar{q}(t)$ is the average concentration through the adsorbent, and

$$\bar{q} = \frac{3}{r_c^3} \int_0^{r_c} q\, r^2\, \mathrm{d}r \tag{5}$$

where q equals the sorbed mass (per unit volume of sorbent), $\bar{q}$ is the average amount adsorbed in a pellet or particle, q_0 is the adsorption capacity at initial time ($t = 0$), q_t is the amount adsorbed at time t, M_∞ is the total mass uptake at a gas-phase concentration of C_0 (inlet concentration of gas-phase), M_t is the mass uptake at time t, and r_0 is the crystalline radius. The concentration of VOCs was determined by gas chromatograph. The VOC sorbed mass (q, q_t, M_t, M_∞, etc.) was measured by an electric balance and calculations, and $\bar{q}$ was obtained by calculations.

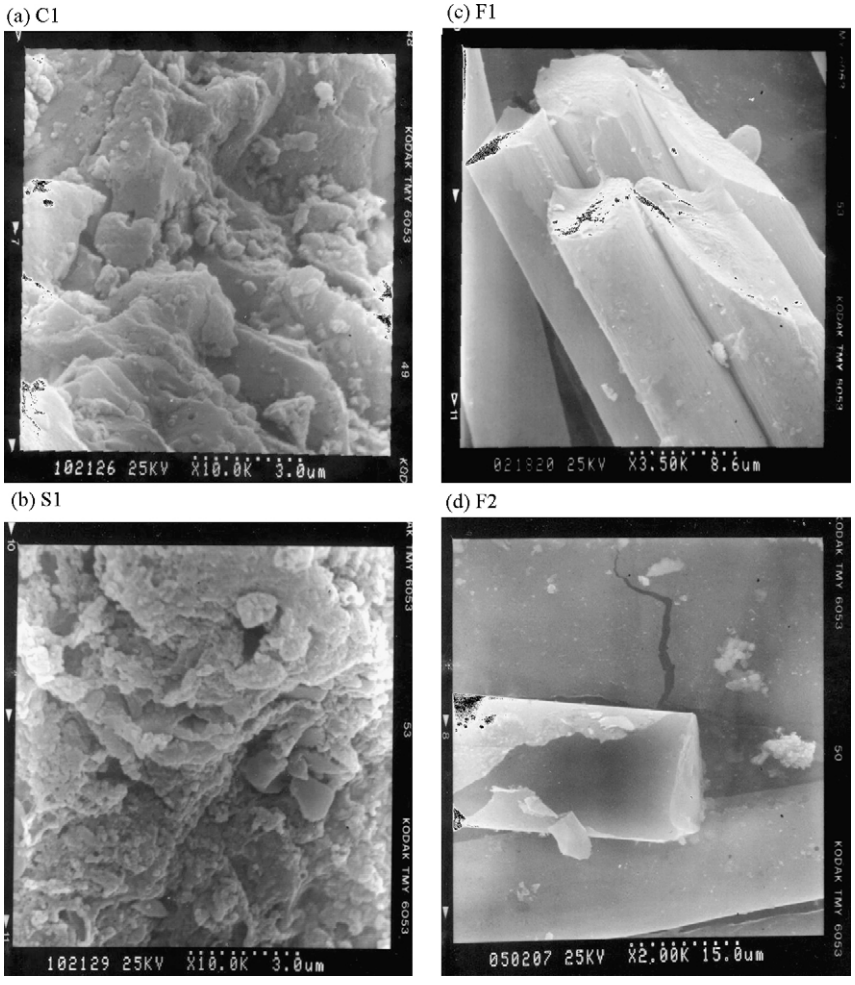

Fig. 1. SEM photographs of different adsorbents.

Table 1
Physical characteristics of adsorbents ($n = 5$)

Adsorbents	SA	PV (cm^3/g)	MA (m^2/g)	MP (cm^3/g)	PD (Å)
C1	807 ± 17	0.42 ± 0.01	520 ± 17	0.23 ± 0.01	20.7 ± 0.74
S1	757 ± 55	0.45 ± 0.05	460 ± 43	0.20 ± 0.02	26.5 ± 0.87
F1	832 ± 29	0.40 ± 0.01	495 ± 120	0.22 ± 0.04	17.2 ± 0.13
F2	1518 ± 148	0.72 ± 0.05	783 ± 83	0.39 ± 0.10	19.1 ± 0.25

SA: surface area, PV: pore volume, MA: micropore area, MP: micropore volume and PD: pore diameter, five samples were analyzed for every adsorbent.

3. Results and discussion

3.1. Physicochemical characteristics

3.1.1. SEM photograph

Fig. 1 shows the SEM photographs of the four kinds of adsorbents used in this study. An irregular surface was found on C1 and S1. In addition, the carbon fiber was cylindrical in shape, but the fiber diameter of F2 (about 18 μm) was larger than that of F1 (about 7.2 μm).

3.1.2. Surface area

Table 1 gives the surface area, micropore area, pore volume, micropore volume, and pore diameter of the adsorbents. The surface area, micropore area, pore volume, and micropore volume of F2 were significantly larger than those of the others. The micropore area contributed over 50% of the specific surface area. The pore diameter in activated carbon fiber was more uniform than that of the granular adsorbents, which could be caused by the characteristics of the raw material and the manufacturing processes.

3.1.3. Pore volume distribution

Fig. 2 shows the pore volume distribution of the adsorbents. The pore size ranged from 200 to 800 Å and from 20 to 90 Å, which contributed a substantial amount of the pore volume of S1. S1 revealed a high mesopore portion in the pore volume. C1, F1, and F2 were mainly micropore. But F2 evidenced a peak in the mesopore range of 20–40 Å.

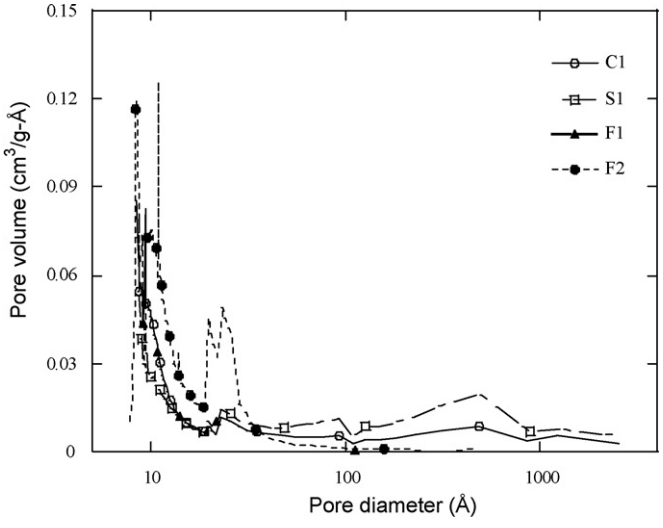

Fig. 2. Pore volume distributions of different adsorbents.

Table 2
Surface functional groups of adsorbents ($n = 5$)

Adsorbents	Carboxyl	Lactone	Phenolic	Carbonyl	Basic
C1	4 ± 2	31 ± 3	4 ± 2	60 ± 4	55 ± 6
S1	50 ± 6	24 ± 2	27 ± 3	ND	70 ± 11
F1	ND	ND	ND	242 ± 12	142 ± 9
F2	ND	11 ± 3	12 ± 2	212 ± 8	134 ± 12

ND: not detectable, five samples were analyzed for every adsorbent.

3.1.4. Ash content

Ash content in C1, S1, F1, and F2 was 4.8%, 11%, 0.2%, and 0.05%, respectively. Results indicated that the raw material of S1 was more complex; therefore, the ash content was higher than that of the others. Activated carbon fibers are made by pitch and coal, yielding almost pure carbon, which leaves only a small amount of ash in the fibers.

3.1.5. pH

The pH of C1, S1, F1, and F2 was 4.6, 5.6, 7.0, and 7.9, respectively. The surface of C1 and S1 tended to be acidic, while the activated carbon fibers tended to be neutral or basic.

3.1.6. Surface functional groups

Table 2 gives the surface oxygenated functional groups of the adsorbents. Carbonyl and lactone were the major surface oxygen functional groups of C1. The carbonyl group was also the major oxygen functional group of activated carbon fiber, contributing over 90%. The surface functional groups of the S1 adsorbent were different from the others; the sequence of its oxygen functional groups was carboxyl > phenolic > lactone. The sludge adsorbent was made from microorganisms, which may be one of the reasons for there being more complex oxygen functional groups on S1 than on the other adsorbents. The sequence of basic functional groups on the adsorbents was F1 > F2 > S1 > C1. Based on the oxygen surface functional groups, the surface of activated carbon fibers was less polar than that of activated carbon and of sludge adsorbent.

3.2. Adsorption capacity of acetone, chloroform and acetonitrile

Fig. 3 shows the adsorption capacity of acetone. While the acetone influent concentration ranged from 80 to 6900 ppm, the adsorption capacity of C1, S1, and F1 was 21–167 mg/g, and

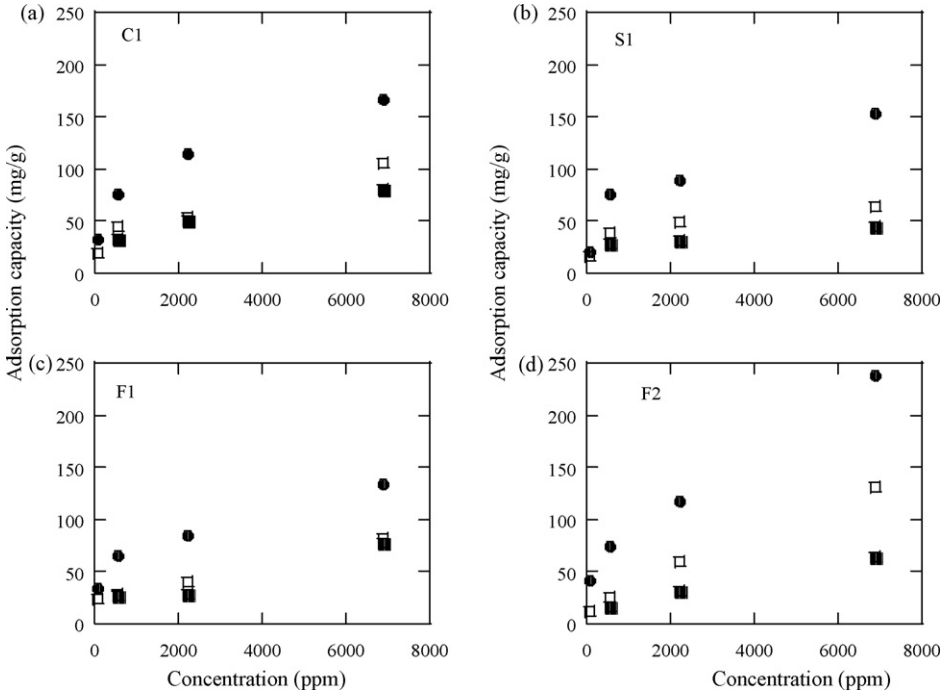

Fig. 3. Adsorption capacity of acetone on different adsorbents and at different temperatures (●: 30 °C, □: 50 °C, and ■: 80 °C).

the adsorption capacity of F2 was about twice that of the other adsorbents. When the adsorption temperature increased to 60°C, the average adsorption capacity of the various concentrations decreased to 0.42–0.57 of the adsorption capacity at 30 °C. In addition, the adsorption capacity at 80 °C was 0.25–0.45 that at 30 °C. When the adsorption temperature increased, the acetone adsorption capacity reduction was high on the F2 adsorbent.

Table 3 gives adsorption capacities of acetonitrile and chloroform on different adsorbents and at different temperatures. The influent concentration of acetonitrile ranged from 43 to 2700 ppm. At an adsorption temperature of 10 °C and an influent concentration of 2700 ppm, the adsorption capacity of C1, S1 and F1 was in the vicinity of 100 mg/g, while that of F2 was 130 mg/g. The increased adsorption temperature corresponding to the reduction of adsorption capacity was significant for all adsorbents. These adsorbents could not effectively capture CH_3CN at high temperature (>50 °C) and low concentration (<300 ppm). Low-temperature adsorption was necessary for using these adsorbents to control acetonitrile vapor.

The influent concentration of chloroform ranged from 90 to 7800 ppm. The adsorption capacity of chloroform at 30 °C ranged from 146 to 373 mg/g on C1, from 70 to 244 mg/g on S1, from 74 to 235 mg/g on F1, and from 128 to 600 mg/g on F2. When the adsorption temperature increased to 80 °C, the adsorption capacity was reduced from that at 30 °C as follows: 7–67% for C1, 17–38% for S1, 5–74% for F1, and 12–42% for F2. While increases in temperature reduce the adsorption capacity at all concentrations, this effect is more pronounced at low concentration than at high concentration.

The adsorption capacity of chloroform on C1 was higher than that on F1. Generally, the affinity of $CHCl_3$ (low dipole moment: 1.1 debyes)-F1 (relative non-polar surface: carbonyl

Table 3
Adsorption capacities of acetonitrile and chloroform on different adsorbents and at different temperatures

Concentration (ppm)	C1				S1				F1				F2			
	10 °C	30 °C	50 °C	80 °C	10 °C	30 °C	50 °C	80 °C	10 °C	30 °C	50 °C	80 °C	10 °C	30 °C	50 °C	80 °C
Acetonitrile																
43	16	10	7	4	60	15	8	Nil	25	12	7	3	20	15	2	Nil
310	22	18	15	8	65	17	10	5	30	18	15	5	27	22	2	2
880	62	43	16	11	81	34	18	14	42	33	22	9	32	38	10	5
2700	100	76	43	14	92	41	20	18	97	56	24	21	130	80	25	10
Chloroform																
90	–	146	56	10	–	70	22	12	–	74	54	4	–	128	30	16
590	–	205	96	94	–	91	59	30	–	151	86	51	–	243	115	97
2370	–	284	206	147	–	154	74	56	–	227	161	112	–	416	233	142
7800	–	373	284	251	–	244	126	93	–	235	220	173	–	600	396	251

Adsorption capacity of chloroform on different adsorbents was not available at 10 °C.

Table 4
Typical adsorption equations for acetone, acetonitrile and chloroform at 30 °C

Adsorbents	Freundlich $q = kC^{1/n}$[a]									Langmuir $q = q_m(KC/(1+KC))$[a]								
	Acetone			Acetonitrile			Chloroform			Acetone			Acetonitrile			Chloroform		
	k[b]	n[b]	r^2[b]	k[b]	n[b]	r^2[b]	k[b]	n[b]	r^2[b]	K[b]	q_m[b,c]	r^2[b]	K[b]	q_m[b]	r^2[b]	K[b]	q_m[b]	r^2[b]
C1	7.1	2.8	0.99	1.3	2.0	0.96	55	4.7	1.0	0.004	0.13	0.97	0.007	0.04	0.87	0.01	0.29	0.85
S1	3.8	2.3	0.94	5.0	3.8	0.85	18	3.5	0.95	0.02	0.13	0.99	0.02	0.03	0.59	0.009	0.15	0.73
F1	9.8	3.4	0.99	2.6	2.7	0.95	24	3.7	0.93	0.007	0.10	0.93	0.01	0.03	0.80	0.005	0.22	0.98
F2	7.5	2.7	0.97	2.9	2.5	0.92	26	2.8	1.0	0.006	0.13	0.88	0.01	0.04	0.77	0.004	0.43	0.94

[a] Adsorption equations.
[b] Parameters.
[c] q_m, g-adsorate/g-adsorbent.

group) is higher than that of $CHCl_3$-C1 (lactone and carbonyl groups on the surface), but it was not reflected in the enhancement of adsorption capacity. Therefore, it can be concluded that the surface functional group of the adsorbent may not be an important factor in chloroform adsorption. The physical characteristics, i.e., micropore area and pore volume distribution, may have a greater effect on the adsorption capacity of adsorbents than the surface oxygenated functional groups, a finding that is similar to the results of Díaz et al. [22].

Based on the adsorption capacity of acetonitrile at different concentrations and temperatures, the average adsorption capacity ratio of S1 was 0.8–2.2 times that of C1, 0.85–1.8 times that of F1, and 0.8–2.9 times that of F2. Particularly at low concentration (<310 ppm) and low temperature (<30 °C), the adsorption capacity of S1 was higher than that of the other adsorbents. The results of this study suggest that sludge adsorbent could be used for polar adsorbates and low concentration at room temperature.

The capacity of chloroform to adsorb S1 was 0.52 that of C1, 0.83 that of F1, and 0.45 that of F2. The dipole moment of $CHCl_3$ (1.1 debyes) is weaker than that of acetonitrile (3.3 debyes), and it may be one of the factors, in addition to pore characteristics, affecting the adsorption capacity on the more polar surface of S1.

The capacity of acetone to adsorb S1 is 0.78 that of C1, 0.97 that of F1, and 0.98 that of F2. Sludge adsorbent, which represents a reuse of waste, can be regarded as an environmentally friendly material for the control of VOCs. In addition, based on the adsorption capacity ratio, the results could reflect the more polar surface of the adsorbent (i.e., S1) that could be selected for acetone adsorption.

The larger molecular weight is associated with high adsorption capacity in acetonitrile and chloroform. In addition, the physical characteristics (i.e., specific surface area and pore volume distribution, etc.) seem to be more important to adsorption in this study. The temperature could have a greater effect on the adsorption of acetonitrile, as its low adsorption energy promotes molecular desorption at high temperature (high temperature increases the entropy in the system).

This study investigated in detail the physical and chemical characteristics of adsorbents and adsorbates. Further work is needed to address the quantitative effects of the physical and chemical characteristics of adsorbents on adsorption capacity. The selected adsorbents are highly active sites. Therefore, the physicochemical characteristics of the adsorbents, i.e., pore size distribution, specific surface area, etc. are important factors for adsorption. But for adsorption of gas (small molecules), the micropore characteristics are more important than the mesopore and macropore characteristics. In addition, the physical characteristics of the adsorbent are more important than the surface oxygen functional group on the adsorbent for non-polar gases sorbed on the adsorbent. Furthermore, the interaction of adsorbent and adsorbate is also a key factor in adsorption capacity. The operation conditions, i.e., influent flow rate, concentration, temperature, etc., affect the adsorption capacity. High concentration and low influent flow rate are associated with high adsorption capacity. Generally, adsorption is an exothermic reaction due to the fact that when a molecule mixes in gas, it evidences a higher degree of disorder than when it is adsorbed on the adsorbent surface and the entropy is increased, revealing an exothermic process. Therefore, the increase the temperature corresponds to the decrease in adsorption capacity.

3.3. Adsorption isotherm

The Freundlich, Langmuir, and Dubinin–Radushkevich (D–R) equations were selected for the adsorption isotherm. Table 4 shows the parameters of the Freundlich and Langmuir isotherms that could be used for the adsorption design of various adsorbents. Based on the difference of adsorption capacity between experimental measurements and adsorption isotherm calculations, the Freundlich isotherm (average absolute difference of 10–18% for three adsobates) was smaller than the D–R (11–31%) and Langmuir (16–28%) isotherms (data not shown). The higher agreement of Freundlich's model is due to its empirical character.

A considerable difference was observed between adsorption isotherms and experimental measurements with acetonitrile. For the D–R model, the difference of acetonitrile was about three times that of acetone and chloroform. Small molecules (low Van der Waals forces) are not easy to adsorb at low concentrations, which may be one of the reasons for the major difference found with acetonitrile. High temperatures (especially higher than the boiling point of adsorbate) and high entropy corresponded to a high variation of adsorption capacity.

Based on the theory of micropore volume filling to derive the Dubinin–Astakhov (D–A) and D–R equations, the detail is as

Table 5
Adsorption characteristic energy (kJ/mole) of adsorbates on adsorbents

Adsorbents	Chloroform	Acetonitrile	Acetone
C1	16.7 ± 3.5	21.8 ± 3.7	19.5 ± 0.94
S1	16.9 ± 1.1	28.7 ± 7.1	21.6 ± 4.3
F1	15.9 ± 3.3	23.2 ± 1.5	21.3 ± 2.4
F2	14.4 ± 1.2	19.2 ± 1.9	16.9 ± 1.1

follows:

$$\text{D–A equation}: \quad W = W_0 \exp\left[-\left(\frac{A}{\beta}E_0\right)^n\right] \tag{6}$$

where $A = RT\ln(P_0/P)$, when $n = 2$ the D–A equation could be shown as D–R equation:

$$\ln(W) = \ln(W_0) - \left(\frac{A}{\beta E_0}\right)^2 \tag{7}$$

where E_0 is the characteristic energy, and β is the affinity coefficient (benzene is a reference vapor).

Table 5 shows the adsorption characteristic energy of adsorbates on adsorbents. According to the volume filling of micropore theory, the smaller the E_0, the easier it is for the adsorbates to adsorb onto the adsorbents [23]. Results for the adsorption characteristic energy were 14.4–16.9 kJ/mole for chloroform, 19.2–28.7 kJ/mole for acetonitrile, and 16.9–21.5 kJ/mole for acetone. Wang et al. [24] used activated carbon to adsorb chloroform and reported a characteristic adsorption energy of 13.3–15.6 kJ/mole. The adsorption energy was in the range of this study. The adsorption energy of acetone in this study was also similar to other measurements in the literature [25–27]. A low adsorption characteristic energy was measured for F2, which may be attributed to the fact that adsorbates are more easily sorbed on carbon fiber. On the other hand, a more polar adsorbent surface (i.e., sludge adsorbent) could account for the high adsorption characteristic energy for these polar molecules.

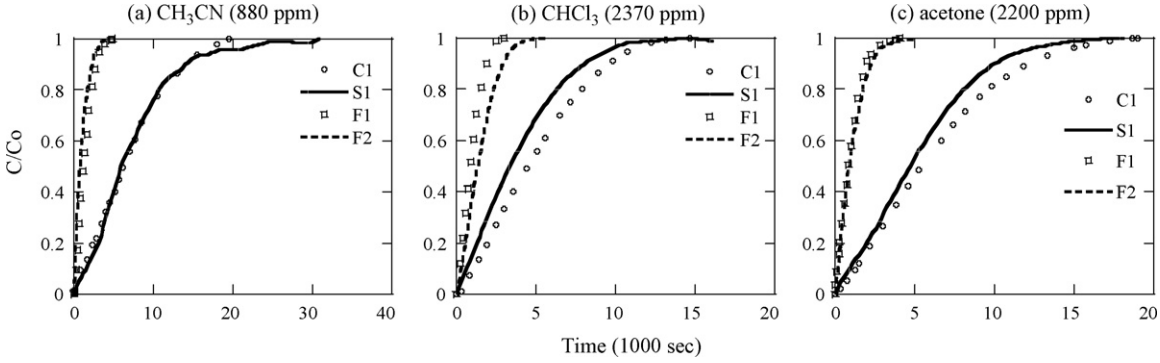

Fig. 4. Typical adsorption kinetic curves of CH_3CN and $CHCl_3$ on different adsorbents.

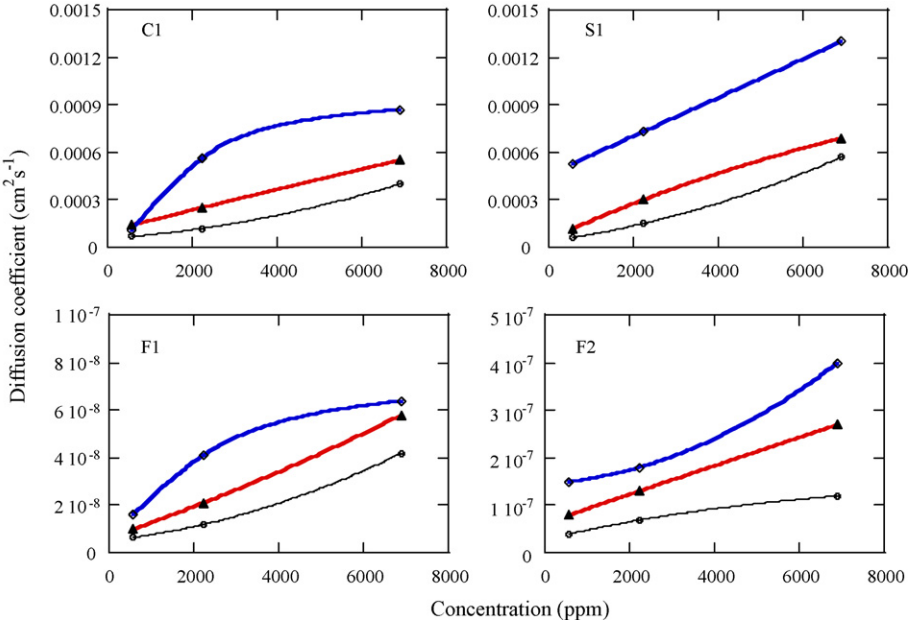

Fig. 5. Diffusivity of acetone on different adsorbents and at different temperatures (◯: 30 °C, ▲: 50 °C and ◊: 80 °C).

Table 6
Diffusivity of acetonitrile and chloroform on different adsorbents and at different temperatures

Concentration (ppm)	C1			S1			F1			F2		
	30° C	50° C	80° C	30° C	50° C	80° C	30° C	50° C	80° C	30° C	50° C	80° C
Acetonitrile												
310	5.6×10^{-5}	6.7×10^{-5}	1.1×10^{-4}	4.9×10^{-5}	8.5×10^{-5}	3.0×10^{-4}	3.6×10^{-9}	7.1×10^{-9}	1.4×10^{-8}	1.4×10^{-8}	2.1×10^{-8}	8.4×10^{-7}
880	7.3×10^{-5}	8.5×10^{-5}	3.4×10^{-4}	1.1×10^{-4}	1.5×10^{-4}	5.1×10^{-4}	6.1×10^{-9}	1.1×10^{-8}	3.0×10^{-8}	6.2×10^{-8}	1.5×10^{-7}	2.7×10^{-7}
2700	1.7×10^{-4}	2.5×10^{-4}	4.7×10^{-4}	3.4×10^{-4}	7.4×10^{-4}	2.7×10^{-4}	8.8×10^{-9}	2.3×10^{-8}	3.7×10^{-8}	8.9×10^{-8}	2.3×10^{-7}	3.9×10^{-7}
Chloroform												
590	4.4×10^{-5}	1.4×10^{-4}	5.8×10^{-4}	7.9×10^{-5}	1.5×10^{-4}	2.1×10^{-4}	3.2×10^{-9}	4.6×10^{-9}	8.7×10^{-9}	1.4×10^{-8}	4.2×10^{-8}	5.0×10^{-8}
2370	7.6×10^{-5}	1.8×10^{-4}	8.5×10^{-4}	1.9×10^{-4}	2.8×10^{-4}	4.0×10^{-4}	1.0×10^{-8}	1.6×10^{-8}	2.1×10^{-8}	4.5×10^{-8}	9.0×10^{-8}	1.5×10^{-7}
7800	1.2×10^{-4}	2.5×10^{-4}	12×10^{-4}	6.8×10^{-4}	8.0×10^{-4}	9.9×10^{-4}	1.6×10^{-8}	3.0×10^{-8}	4.0×10^{-8}	8.7×10^{-8}	1.5×10^{-7}	3.1×10^{-7}

3.4. Diffusivity of acetone, acetonitrile and chloroform

Fig. 4 shows the typical chloroform and acetonitrile adsorption kinetic curves of the various adsorbents. Results indicated that the adsorption rate of activated carbon fiber reached equilibrium faster than granular activated carbon and sludge adsorbent, which may be due to the fact that the diameter of the fibers is smaller than those of granular adsorbents.

Fig. 5 and Table 6 show the micropore diffusion coefficient of chloroform, acetonitrile and acetone on various adsorbents. The sequence of CH_3CN diffusivity obtained was S1 (10^{-4} to $10^{-3}\,cm^2\,s^{-1}$) > C1 (10^{-5} to $10^{-4}\,cm^2\,s^{-1}$) > F2 (10^{-8} to $10^{-7}\,cm^2\,s^{-1}$) > F1 (10^{-9} to $10^{-8}\,cm^2\,s^{-1}$). In addition, the sequence of chloroform diffusivity was C1 ($10^{-4}\,cm^2\,s^{-1}$) ≈ S1 ($10^{-4}\,cm^2\,s^{-1}$) > F2 (10^{-8} to $10^{-7}\,cm^2\,s^{-1}$) > F1 (10^{-9} to $10^{-8}\,cm^2\,s^{-1}$). The sequence of acetone diffusivity was S1 (10^{-4} to $10^{-3}\,cm^2\,s^{-1}$) ≈ C1 (10^{-4} to $10^{-3}\,cm^2\,s^{-1}$) > F2 (10^{-8} to $10^{-7}\,cm^2\,s^{-1}$) > F1 (10^{-9} to $10^{-8}\,cm^2\,s^{-1}$). Generally, the diffusivity of CH_3CN and acetone was higher than that of $CHCl_3$, which may be caused by the high molecular weight of $CHCl_3$. High adsorption temperature and concentration could enhance diffusivity, especially in the large-pore-diameter adsorbents (C1 and S1). When the adsorption temperature increased from 30 to 80 °C, the diffusivity increased about one order. The low diffusivity of adsorbates in fibers may be attributed to the small pore diameter and pore structure.

4. Conclusions

Generally, the adsorption capacity of chloroform, acetonitrile, and acetone was higher on F2 than on the others. The adsorption rate of activated carbon fiber was higher than that of activated carbon and sludge adsorbent due to the small fiber diameter. In addition, the surface area of the fibers was higher than those of the others. The adsorption capacity of acetonitrile, chloroform, and acetone on sludge adsorbent was 0.8–2.9, 0.45–0.83, and 0.78–0.98 times that of the other adsorbents. Results indicate that sludge adsorbent could be used for VOC adsorption, especially in more polar adsorbates and at lower temperatures. Based on the D–R equation, the adsorption characteristic energy was 14.4–16.9 kJ/mole for chloroform, 19.2–28.7 kJ/mole for acetonitrile, and 16.9–21.5 kJ/mole for acetone. According to the adsorption kinetic curves, the micropore diffusion coefficient of VOC on activated carbon and sludge adsorbent (10^{-5} to $10^{-4}\,cm^2\,s^{-1}$) was higher than activated carbon fibers (10^{-8} to $10^{-7}\,cm^2\,s^{-1}$). The pore size of carbon fibers is smaller than those of both activated carbon and sludge adsorbent, corresponding to the smaller diffusion coefficient of activated carbon fibers.

Acknowledgements

The authors express their sincere thanks to the National Science Council, Taiwan, ROC (Contract NSC 94-2211-E-039-07 and 95-2211-E-039-012) for funding this study.

References

[1] H.C. Shin, J.W. Park, K. Park, H.C. Song, Removal characteristics of trace compounds of landfill gas by activated carbon adsorption, Environ. Pollut. 119 (2002) 227–236.

[2] A. Giaya, R.W. Thomspon, Single-component gas phase adsorption desorption studies using a tapered element oscillating microbalance, Microporous Mesoporous Mater. 55 (2002) 265–274.

[3] H. Tamon, M. Okzaki, Influence of acidic surface oxides of activated carbon on gas adsorption characteristics, Carbon 34 (1996) 741–746.

[4] I. Abe, T. Fukuhara, J. Maruyama, H. Tatsumoto, Preparation of carbonaceous adsorbents for removal of chloroform from drinking water, Carbon 39 (2001) 1069–1073.

[5] P.C. Chiang, J.H. You, Use of sewage sludge for manufacturing adsorbents, Can. J. Chem. Eng. 65 (1987) 922–927.

[6] G.Q. Lu, J.C.F. Low, C.Y. Liu, A.C. Lua, Surface area development of sewage sludge during pyrolysis, Fuel 74 (1995) 344–348.

[7] S. Jeyaseelan, G.Q. Lu, Development of adsorbent/catalyst from municipal wastewater sludge, Water Sci. Technol. 34 (1996) 499–505.

[8] K.L. Foster, R.G. Fuerman, J. Economy, S.M. Larson, M.J. Rood, Adsorption characteristics of trace volatile organic compounds in gas streams onto activated carbon fibers, Chem. Mater. 4 (1992) 1068–1073.

[9] H. Rong, Z. Ryu, J. Zheng, Y. Zhang, Effect of air oxidation of rayon-based activated fibers on the adsorption behavior for formaldehyde, Carbon 40 (2002) 2291–2300.

[10] I.N. Ermolenko, I.P. Lyubliner, N.V. Guiko, Chemically Modified Carbon Fibers And Their Applications, VCH, Weinheim, 1990, Translated by EP Titovets.

[11] K.P. Singh, D. Mohan, G.S. Tandon, G.S.D. Gupta, Vapor-phase adsorption of hexane and benzene on activated carbon fabric cloth: equilibria and rate studies, Ind. Eng. Chem. Res. 41 (2002) 2480–2486.

[12] Z. Hashiho, M. Rood, L. Botich, Microwave-swing adsorption to capture and recover vapors from air streams with activated carbon fiber cloth, Environ. Sci. Technol. 39 (2005) 6851–6859.

[13] H.L. Chiang, K.H. Lin, C.Y. Chen, C.G. Chao, C.S. Hwu, N. Lai, Adsorption characteristics of benzene on biosolid adsorbent and commercial activated carbons, J. Air Waste Manage. Assoc. 56 (2006) 591–600.

[14] S. Brubauer, H.P. Emmett, E. Teller, Adsorption of gas in multimolecular layers, J. Am. Chem. Soc. 60 (1938) 309–319.

[15] E.P. Barrett, L.S. Joyner, P.P. Halenda, The determination of pore volume and area distributions in porous substances. I. Computations from nitrogen isotherm, J. Am. Chem. Soc. 73 (1951) 373–380.

[16] B.C. Lippens, de BoerF J.H., Studies on pore system in catalysts. V. The *t* method, J. Catal. 4 (1965) 319–323.

[17] W.D. Harkins, G. Jura, Surfaces of solids XIII: a vapor adsorption method for the determination of the area of a solid without the assumption of a molecular area and the areas occupied by nitrogen and other molecules on the surface of a solid, J. Chem. Phys. 66 (1944) 1366–1377.

[18] H.P. Boehm, Chemical identification of surface groups, in: D.D. Eley, H. Pines, P.B. Weisz (Eds.), Advances in Catalysis, vol. 16, Academic Press, New York, 1966, p. 179.

[19] T. Fabish, D.E. Schleifer, Surface chemistry and carbon black work function, Carbon 22 (1984) 19–38.

[20] K. Kinoshita, Carbon: Electrochemical and Physicochemical Properties, Wiley, New York, 1988.

[21] D.M. Ruthven, Principles of Adsorption and Adsorption Processes, John Wiley & Sons, New York, 1984.

[22] E. Díaz, S. Ordóñez, A. Vega, J. Coca, Comparison of adsorption properties of a chemically activated and a steam-activated carbon, using inverse gas chromatography, Microporous Mesoporous Mater. 82 (2005) 173–181.

[23] V. Ponec, Z. Knor, S. Cerny, Adsorption on Solids, The Chemical Rubber Company, Cleveland Ohio, 1974.

[24] G.S. Wang, J.W. Lee, H. Moon, Adsorption of carbon tetrachloride and chloroform on activated carbon at (300.15, 310.15, 320.15, and 330.15) K, J. Chem. Eng. Data 48 (2003) 286–290.

[25] W.H. Lee, P.J. Reucroft, Vapor pressure on coal- and wood-based chemically activated carbons (II) adsorption of organic vapors, Carbon 37 (1999) 15–20.

[26] C.T. Hsieh, J.M. Chen, Adsorption energy distribution model for VOCs onto activated carbons, J. Colloid Interface Sci. 255 (2002) 248–253.

[27] N. Chakrapani, Y.M. Zhang, S.K. Nayak, J.A. Moore, D.L. Carroll, Y.Y. Choi, P. Ajayan, Chemisorption of acetone on carbon nanotube, J. Phys. Chem. B 107 (2003) 9308–9311.